



CHORUS

This is the accepted manuscript made available via CHORUS. The article has been published as:

Modes of Magnetic Resonance in the Spin-Liquid Phase of $\text{Cs}_{2}\text{CuCl}_{4}$

K. Yu. Povarov, A. I. Smirnov, O. A. Starykh, S. V. Petrov, and A. Ya. Shapiro

Phys. Rev. Lett. **107**, 037204 — Published 14 July 2011

DOI: [10.1103/PhysRevLett.107.037204](https://doi.org/10.1103/PhysRevLett.107.037204)

Modes of magnetic resonance in the spin liquid phase of Cs_2CuCl_4

K. Yu. Povarov,^{1,*} A. I. Smirnov,^{1,2} O. A. Starykh,^{3,4} S. V. Petrov,¹ and A. Ya. Shapiro⁵

¹*P. L. Kapitza Institute for Physical Problems, RAS, 119334 Moscow, Russia*

²*Moscow Institute for Physics and Technology, 141700, Dolgoprudny, Russia*

³*Department of Physics and Astronomy, University of Utah, Salt Lake City, Utah 84112, USA*

⁴*Max-Planck-Institut für Physik Komplexer Systeme, D-01187 Dresden, Germany*

⁵*A.V.Shubnikov Institute of Crystallography, RAS, 119333 Moscow, Russia*

We report the observation of a frequency shift and splitting of the electron spin resonance (ESR) mode of the low-dimensional $S = 1/2$ frustrated antiferromagnet Cs_2CuCl_4 in the spin-correlated state above the ordering temperature 0.62 K. The shift and splitting exhibit strong anisotropy with respect to the direction of the applied magnetic field and do not vanish in zero field. The low-temperature evolution of the ESR is a result of modification of the one-dimensional spinon continuum by the uniform Dzyaloshinskii-Moriya interaction (DM) within the spin chains.

PACS numbers: 76.30.-v, 75.40.Gb, 75.10.Jm

Relentless search [1] for fractionalized spin-1/2 magnetic excitations - spinons - has yielded several clear-cut ‘sightings’ of them in magnetic insulators. The experimental probes include inelastic neutron scattering (INS) [2–4], thermal conductivity [5, 6] and photoemission [7]. Most of the investigated materials possess a very high degree of one-dimensionality (1D) making them a natural ‘habitat’ for spinons, which are extended spin-1/2 domain-wall excitations. More recently it has been realized that 1D spinons can be present in a higher-dimensional settings as well [8–11], provided that spin interactions are sufficiently frustrated to allow for a wide intermediate (in temperature and/or energy) window in which the 1D scaling can develop. A well understood example is provided by amazingly versatile triangular lattice antiferromagnet Cs_2CuCl_4 INS studies of which uncovered an extensive two-spinon continuum [12, 13]. Most of the INS spectral intensity is found to be carried by spinons with large momenta. Our work describes an entirely novel, ESR-based way to probe the width and the shape of the spinon continuum at small momenta. In doing so we establish a rather unexpected connection of the problem of spinon excitations in the Heisenberg spin chains subject to the *uniform* Dzyaloshinskii-Moriya (DM) interaction with that of electrons in semiconductor heterostructures subject to the spin-orbital interaction of Rashba-type [14–16].

Cs_2CuCl_4 realizes distorted triangular lattice with strong exchange J along the base of the triangular unit and weaker exchange integral $J' = 0.34J$ along lateral sides of the triangle. The material orders below $T_N = 0.62$ K into a long-range 3D spiral state [12]. The T_N is far below the Curie-Weiss temperature $T_{CW} = 4$ K. In the intermediate temperature range $T_N < T < T_{CW}$ a spin-liquid phase with strong in-chain spin correlations takes place. Both the dynamic spin structure factor [8] and the low-temperature phases [17] of Cs_2CuCl_4 are well described by a quasi-1D model of weakly coupled spin $S = 1/2$ chains, extended in [9] to include crucial

symmetry-allowed DM interactions between the spins.

ESR is well known as a method providing fine details of spin excitation spectra at small momenta in both ordered and paramagnetic [18, 19] phases. Here we uncover dramatic sensitivity of the ESR and spinon spectra to the *uniform* DM interaction in the spin-liquid phase of Cs_2CuCl_4 . We observe and *explain* splitting of the ESR mode into two modes with lowering the temperature, as well as its remarkable polarization anisotropy.

The crystal samples were grown by two methods. First set of samples was prepared by the crystallization from the melt of a stoichiometric mixture of CsCuCl_3 and CsCl in an ampule, which was slowly pulled from the hot ($T = 520^\circ\text{C}$) area of the oven. The second method was crystallization from solution [20]. The room temperature crystal lattice parameters for both sets of crystals are $a = 9.756$ Å, $b = 7.607$ Å, $c = 12.394$ Å. The samples obtained by last method have natural faces and are lengthened along b -axes. Both sets of crystals demonstrated identical ESR signals. The study in the frequency range 9-90 GHz was performed with a set of homemade spectrometers equipped with cryomagnets. The resonance lines were taken at the fixed frequency, as dependences of microwave power, transmitted through the resonator, on the external magnetic field. Temperatures down to 1.3 K (0.4 K), were obtained by pumping vapor of ^4He (^3He), correspondingly. Cooling down to 0.1 K was achieved with the help of a dilution cryostat Kelvinox-400.

At temperatures above $T = 10$ K we observe conventional paramagnetic resonance with a single narrow line corresponding to g -factor values $g_a = 2.20 \pm 0.02$, $g_b = 2.08 \pm 0.02$, $g_c = 2.30 \pm 0.02$. These g -factor values agree well with those reported earlier at $T = 300$ K and 77 K [21], and, for g_c , at $T = 4.2$ K [22].

Significant evolution of the ESR spectrum was found on cooling below 6 K. This evolution depends strongly on the microwave frequency ν and orientation of the external magnetic field \mathbf{H} . (*i*) For $\mathbf{H} \parallel \mathbf{b}$, we observe a single Lorentzian line shifting with cooling to lower fields

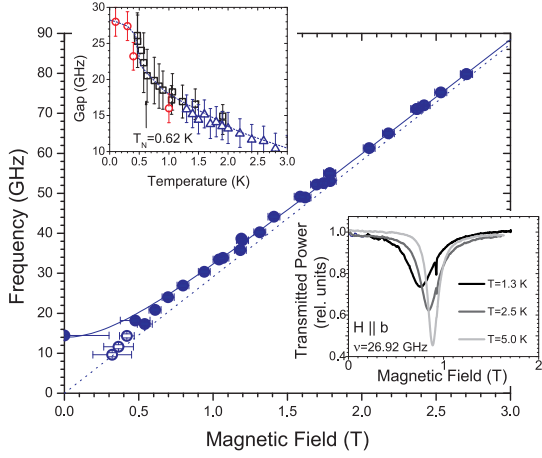


FIG. 1. (Color online). ESR frequency at $T = 1.3$ K for $H \parallel \mathbf{b}$. Dotted line is paramagnetic resonance with $g = 2.08$, solid line – theory (see text). Empty circles stand for resonances losing intensity with cooling. Upper insert: gap vs temperature, various symbols correspond to different cryostats. Lower insert: evolution of the resonance line with cooling.

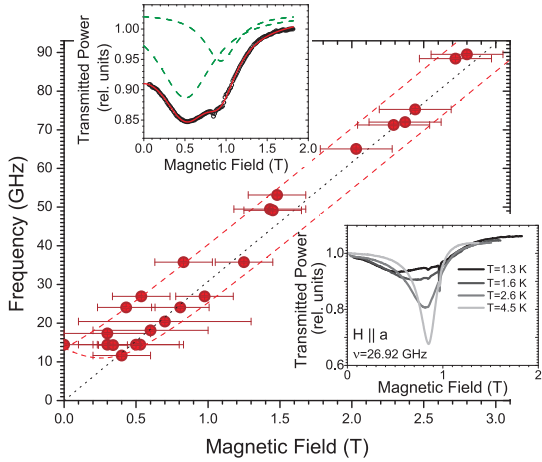


FIG. 2. (Color online). ESR frequencies at $T = 1.3$ K for $H \parallel \mathbf{a}$. Dotted line is paramagnetic resonance with $g = 2.20$, dashed line – theory (see text). Upper insert: lineshape at $T = 1.3$ K, $\nu = 27$ GHz. Points – experimental data, solid line is the result of a fit by the sum of two Lorentzians (dashed lines). Lower insert: evolution of the resonance line with cooling.

(see Fig. 1). At $\nu=14$ GHz the resonance field is near zero at $T = 1.3$ K. At lower frequencies, we observe a strong decrease of the intensity with cooling, and no visible shift from the paramagnetic resonance field, in contrast to ESR lines taken at $\nu > 17$ GHz, which exhibit a shift and do not lose intensity on cooling. At $\nu=9$ GHz the integral intensity at $T=1.3$ K is a half of that at $T=4$ K. The resonant frequencies above 14 GHz may be well fitted by the frequency-field relation of an ordered anti-

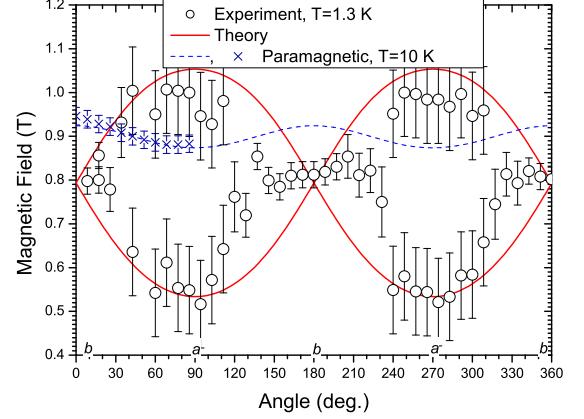


FIG. 3. (Color online). The angular dependence of the resonance field H_r in the \mathbf{ab} plane for $\nu = 27$ GHz at $T = 1.3$ K. Thick line is the theoretical prediction with $D_a/(4\hbar) = 8$ and $D_c/(4\hbar) = 11$ GHz. The measured values of the resonance field deep in the paramagnetic phase (at $T = 10$ K) are presented by crosses, the dashed line is a theoretical fit of a paramagnetic resonance with $g_{a,b,c}$ of Cs_2CuCl_4 .

ferromagnet with “gap” $\Delta/(2\pi\hbar) = 14$ GHz at $T=1.3$ K,

$$2\pi\hbar\nu = \sqrt{(g\mu_B H)^2 + \Delta^2}. \quad (1)$$

(ii) For $\mathbf{H} \parallel \mathbf{a}, \mathbf{c}$, the ESR line strongly broadens on cooling, and its shape distorts, as shown in the inserts of Fig. 2. The absorption at $T=1.3$ K may be fitted by a sum of two Lorentzians, indicating the splitting of the resonance mode. The $\nu(H)$ dependence at $\mathbf{H} \parallel \mathbf{a}$ is presented in Fig. 2. Two modes at $T = 1.3$ K were resolved for measurements in the frequency range 14-50 GHz. Similar splitting was reported previously in [22]. At higher frequencies the splitting is masked by natural linewidth, which prevents the resolution of the doublet, while at lower frequencies the signal becomes too broad. The angular ϕ dependence of the resonance field $\mathbf{H}_r = H(\sin \phi, \cos \phi, 0)$ within the $\mathbf{a} - \mathbf{b}$ plane, taken at $\nu=27$ GHz and $T=1.3$ K, is shown in Fig.3. For $\mathbf{H} \parallel \mathbf{c}$ the splitting of about 0.35 ± 0.1 T is resolved for frequencies 27 and 31 GHz.

(iii) We have also studied polarization dependence of the ESR absorption at $H \rightarrow 0$. Fig.4 shows ESR records at $T = 1.3$ K and $T = 6$ K for different orientations of the microwave and static fields with respect to the crystal axes, but with $\mathbf{h} \perp \mathbf{H}$, at the frequency $\nu = 14$ GHz. At $T \geq 6$ K both the position and the lineshape of the paramagnetic resonance line are the same for all three principal polarizations of the microwave field. However, at $T = 1.3$ K, the absorption in zero field for $\mathbf{h} \parallel \mathbf{b}$ is at least three times more intensive than for $\mathbf{h} \parallel \mathbf{a}, \mathbf{c}$.

The above observations strongly distinguish Cs_2CuCl_4 from other known $S = 1/2$ antiferromagnets such as a conventional 3D magnet and a critical quantum spin

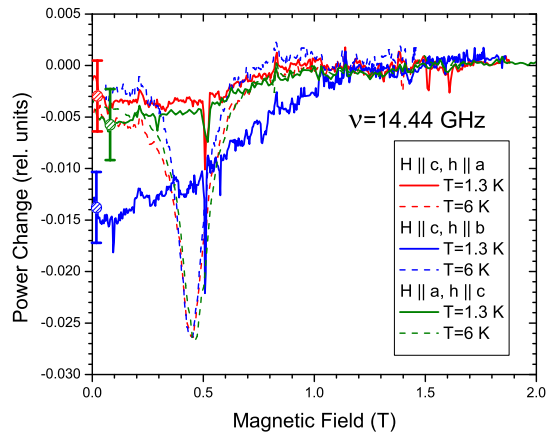


FIG. 4. (Color online). The polarization effect at $\nu = 14.44$ GHz for $H \rightarrow 0$. Circles with error bars show the uncertainty resulting from normalizing the signals to zero absorption at $H > 1.5$ T.

chain. The former exhibits an energy gap which vanishes at the ordering temperature, while the latter shows an ESR shift due to an anisotropic exchange and/or a staggered DM interaction, but only in a presence of the external magnetic field [19, 23]. Unlike Cs_2CuCl_4 , these systems do not exhibit a finite frequency gap (1) for $H=0$ and a direction-dependent splitting of the ESR line, Fig.3, all in the paramagnetic phase.

We now show that all these unusual features follow from a quasi-1D nature of Cs_2CuCl_4 and the uniform structure of the DM interaction. Our Hamiltonian

$$\mathcal{H} = \sum_{x,y,z} (J\mathbf{S}_{x,y,z} \cdot \mathbf{S}_{x+1,y,z} - \mathbf{D}_{y,z} \cdot \mathbf{S}_{x,y,z} \times \mathbf{S}_{x+1,y,z} + g\mu_B \mathbf{H} \cdot \mathbf{S}_{x,y,z}) + \dots \quad (2)$$

contains three terms: the first describes intrachain exchange J (x runs along crystal \mathbf{b} axis), the second – uniform DM interaction $\mathbf{D}_{y,z}$ between chain spins, and the third is the usual Zeeman term, allowing for anisotropic g -factor. The dots stand for the omitted interchain exchange as well as DM interactions on interchain bonds. Detailed symmetry analysis of the allowed DM interactions [9] shows that there are *four* different orientations of the DM vector (see Fig. 6 in [9]) depending on chain's integer coordinates y, z : $\mathbf{D}_{y,z} = D_a(-1)^z \hat{a} + D_c(-1)^y \hat{c}$. Here z indices magnetic $\mathbf{b} - \mathbf{c}$ layers, while y numerates chains within a layer. Crucially, crystal symmetry forbids DM vector to have component along the \mathbf{b} axis [9].

The essence of the observed ESR line splitting can be explained by considering a single Heisenberg chain with uniform DM interaction with vector \mathbf{D} along the local \hat{z} axis, and $\mathbf{H} \parallel \mathbf{z}$ ($\mathbf{D}_{y,z} \rightarrow D\hat{z}$, $\mathbf{H} \rightarrow H\hat{z}$). In this geometry the DM interaction can be gauged away by

position-dependent rotation of *lattice* spins,

$$S_{x,y,z}^+ = \tilde{S}_{x,y,z}^+ e^{i\alpha x}, \quad S_{x,y,z}^z = \tilde{S}_{x,y,z}^z. \quad (3)$$

The rotation angle $\tan(\alpha) = -D/J$ is chosen so as to eliminate the DM coupling from the Hamiltonian. The transformed $\tilde{\mathcal{H}}$ describes spin chain with *quadratic* in D easy-plane anisotropy. To linear in D/J accuracy the ESR response of this model coincides with that of an isotropic Heisenberg chain, detailed study of which is described in Ref.[19]. ESR absorption is determined by the transverse structure factor $\mathcal{S}_{xx}(\omega, \tilde{q}) = \mathcal{S}_{yy}(\omega, \tilde{q})$ of the chain, evaluated at $\tilde{q} = 0$. This is given by the sum of delta-function peaks at frequencies $2\pi\hbar\nu_{R/L} = |\hbar v\tilde{q} \pm g\mu_B H|$, see eq.(3.16) of [19] and Fig.5. Here $v = \pi J a_0 / (2\hbar)$ is the zero-field spinon velocity and a_0 is the lattice spacing. The response in the *original* (unrotated) basis is obtained by un-doing the momentum boost (3), which corresponds to setting $\tilde{q} = D/Ja_0$ in the expression for the structure factor $\mathcal{S}_{xx/yy}$. This immediately implies the splitting of the ESR line into two lines, at frequencies $2\pi\hbar\nu_{R/L} = |g\mu_B H \pm \pi D/2|$ [24]. Note that the splitting $\pi D = \pi(D_a^2 + D_c^2)^{1/2}$ is linear in D which justifies our neglect of the easy-plane anisotropy.

While the four-sublattice structure of the DM vectors makes it impossible to study the $\mathbf{D} \parallel \mathbf{H}$ configuration in Cs_2CuCl_4 , the above argument allows one to immediately understand polarization-dependent absorption (finding *iii*) above) in zero magnetic field, at the frequency $2\pi\nu = \pi D/2\hbar$. Since the microwave absorption is proportional to the square of the microwave field component perpendicular to the effective field, we conclude that configuration with $\mathbf{h} \perp \mathbf{D}$ (that is, $\mathbf{h} \parallel \mathbf{b}$) should result in maximal possible absorption. For \mathbf{h} along the \mathbf{a} (\mathbf{c}) axis, absorption is a factor D_c^2/D^2 (D_a^2/D^2) smaller. Using numerical estimates of $D_{a,c}$ derived below, the absorption for different polarizations should obey the relations: $P_b/P_a \simeq 1.6$ and $P_b/P_c \simeq 2.8$. This agrees qualitatively with our data presented in Fig. 4 – the zero field absorption at $\nu = 14$ and 17 GHz is a factor of 3 more intensive for $\mathbf{h} \parallel \mathbf{b}$ than for $\mathbf{h} \parallel \mathbf{a}, \mathbf{c}$.

To understand our findings (*i*) and (*ii*), one needs to analyze the arbitrary orientation of the \mathbf{H} and \mathbf{D} vectors, which is the problem solved in Ref.[25]. The main physical point of [25] consists in the observation that a uniform DM interaction, much like a spin-orbit Rashba interaction in 2D conductors [14–16], acts on spinon excitations of 1D chains as an internal momentum-dependent magnetic field. Technically, this observation follows from spin-current formulation [24] of the problem (2), which is valid below the strong-coupling temperature scale $T_0 \sim J e^{-\pi S}$ ($S = 1/2$ for the spin chain here)[26]. The spin currents $\mathbf{M}_{R/L}$ represent spin density fluctuations of spinons near the right/left (R/L) Fermi points of a 1D system. It follows that the right and left-moving currents experience *different*, in magnitude and direction, *total* magnetic fields: $\mathbf{B}_R = \mathbf{H} + \hbar v \mathbf{D} / g\mu_B J$ and

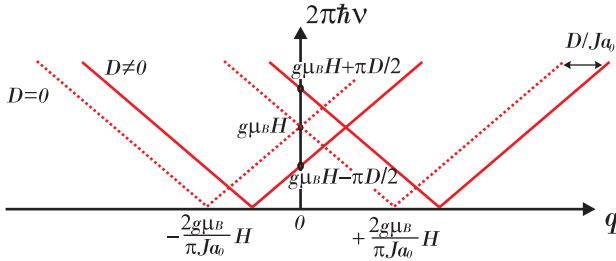


FIG. 5. (Color online). Spinon spectrum of $S = 1/2$ Heisenberg chain for $\mathbf{q} \sim 0$ with (solid lines) and without (dashed lines) DM interaction. When $\mathbf{D} \parallel \mathbf{H}$, momentum is boosted by $q = D/Ja_0$.

$\mathbf{B}_L = \mathbf{H} - \hbar\nu\mathbf{D}/g\mu_B J$. It is then natural that the ESR response of such a chain consists of two peaks at frequencies $2\pi\hbar\nu_{R/L} = g\mu_B B_{R/L}$. [25]

For the Cs_2CuCl_4 -specific configuration of chain DM interactions and $\mathbf{H} = (H_a, H_b, H_c)$ our analysis predicts

$$(2\pi\hbar\nu_R)^2 = (g_b\mu_B H_b)^2 + (g_a\mu_B H_a + (-1)^z \pi D_a/2)^2 + (g_c\mu_B H_c + (-1)^y \pi D_c/2)^2, \quad (4)$$

$$(2\pi\hbar\nu_L)^2 = (g_b\mu_B H_b)^2 + (g_a\mu_B H_a - (-1)^z \pi D_a/2)^2 + (g_c\mu_B H_c - (-1)^y \pi D_c/2)^2, \quad (5)$$

These equations naturally explain the difference between $\mathbf{H} \parallel \mathbf{a}, \mathbf{c}$ and $\mathbf{H} \parallel \mathbf{b}$ situations. For $\mathbf{H} \parallel \mathbf{b}$ the external and the internal DM field are mutually perpendicular and the vector sum $\mathbf{H} \pm \mathbf{D}$ has the same absolute value for both signs. One then finds single ESR frequency $\nu_R = \nu_L$ of the form (1) where the “gap” is in fact an *internal* DM field, $\Delta/(2\pi\hbar) = \sqrt{D_a^2 + D_c^2}/(4\hbar) \approx 14$ GHz, using $D_{a/c}$ values reported below. For $\mathbf{H} \parallel \mathbf{a}, \mathbf{c}$ the DM field has a component along \mathbf{H} and the frequencies of the two spin excitations are different. Solving equations (4,5) at fixed frequency for the magnetic field \mathbf{H} within the $\mathbf{a}-\mathbf{b}$ plane we were able to fit the experimental angular dependence in Fig. 3. In this way we obtained $D_a/(4\hbar) = 8 \pm 2$ and $D_c/(4\hbar) = 11 \pm 2$ GHz, which corresponds to 0.29 ± 0.07 and 0.39 ± 0.07 T. Details of the angular dependence of ESR for field oriented within $\mathbf{a}-\mathbf{c}$ plane are discussed in Ref.[24].

A more detailed comparison between the experiment and the theory would require extending the latter to finite temperatures since the reported measurements are performed in the intermediate temperature range $T_N = 0.62\text{K} < T < T_{CW} = 4\text{K}$. Temperature dependence of the gap Δ for $\mathbf{H} \parallel \mathbf{b}$ in a wider range including T_N is shown in Fig.1. The variation of the gap in the range $1\text{K} < T < 2\text{K}$ is much slower than right near T_N . This supports our main assumption that the reported spectral features of Cs_2CuCl_4 reflect specific spin chain physics which dominates the temperature range $T_N < T < T_{CW}$.

In conclusion, we demonstrated that the uniform DM

interaction, which is a distinctive feature of Cs_2CuCl_4 , results in a new kind of spin resonance in a $S=1/2$ chain antiferromagnet. The observed spectrum is a consequence of the splitting of the chain’s spinon continuum by the internal magnetic field which is produced by the uniform DM interaction. It would be interesting to probe this physics independently via polarized neutron scattering as suggested in Ref.27. We believe that our findings can be extended to higher-dimensional magnetic systems with fractionalized spinon excitations.

We would like to thank K.O. Keshishev for guidance in work with the dilution refrigerator, and L. Balents, S. Gangadharaiah, V.N. Glazkov, M. Oshikawa, and R. Moessner for insightful discussions. We thank RFBR Grant 09-02-736 and NSF Grant No. DMR-0808842 (O.A.S.) for financial support. Part of the work has been performed within the ASG on “Unconventional Magnetism in High Fields” at the MPIPKS (Dresden).

* povarov@kapitza.ras.ru

- [1] L. Balents, Nature **464**, 199 (2010).
- [2] D. C. Dender *et al.*, Phys. Rev. Lett. **79**, 1750 (1997).
- [3] M. B. Stone *et al.*, Phys. Rev. Lett. **91**, 037205 (2003).
- [4] M. Enderle *et al.*, Phys. Rev. Lett. **104**, 237207 (2010).
- [5] N. Hlubek *et al.*, Phys. Rev. B **81**, 020405 (2010).
- [6] T. Kawamata *et al.*, J. Phys. Conf. Ser. **200**, 022023 (2010).
- [7] B. J. Kim *et al.*, Nat. Phys. **2**, 397 (2006).
- [8] M. Kohno, O. A. Starykh, and L. Balents, Nat. Phys. **3**, 790 (2007).
- [9] O. A. Starykh, H. Katsura, L. Balents, Phys. Rev. B **82**, 014421 (2010).
- [10] M. Q. Weng *et al.*, Phys. Rev. B **74**, 012407 (2006).
- [11] D. Heidarian, S. Sorella, F. Becca, Phys. Rev. B **80**, 012404 (2009).
- [12] R. Coldea *et al.*, Phys. Rev. Lett. **86**, 1335 (2001).
- [13] R. Coldea, D. A. Tennant, Z. Tylczynski, Phys. Rev. B **68**, 134424 (2003).
- [14] V. K. Kalevich and V. L. Korenev, JETP Lett. **52**, 230 (1990).
- [15] Z. Wilamowski *et al.*, Phys. Rev. Lett. **98**, 187203 (2007).
- [16] S. M. Frolov *et al.*, Nature **458**, 868 (2009).
- [17] Y. Tokiwa *et al.*, Phys. Rev. B **73**, 134414 (2006).
- [18] K. Katsumata, J. Phys.: Condens. Matter **12**, R589 (2000).
- [19] M. Oshikawa, I. Affleck, Phys. Rev. B **65**, 134410 (2002).
- [20] L. V. Soboleva *et al.*, Kristallografiya **24**, 817 (1981).
- [21] M. Sharnoff, J. Chem. Phys. **44**, 3383 (1964).
- [22] J. M. Schrama *et al.*, Physica B **256-258**, 637 (1998).
- [23] T. Asano *et al.*, Phys. Rev. Lett. **84**, 5880 (2000).
- [24] see *Supplemental material* for more details.
- [25] S. Gangadharaiah, J. Sun, O. A. Starykh, Phys. Rev. B **78**, 054436 (2008).
- [26] C. Buragohain and S. Sachdev, Phys. Rev. B **59**, 9285 (1999).
- [27] D. N. Aristov and S. V. Maleyev, Phys. Rev. B **62**, 751 (2000).